THE ASTROPHYSICAL JOURNAL, 473:219–229, 1996 December 10

CO OBSERVATIONS AND A NEW INTERPRETATION OF THE ANOMALOUS ARMS OF NGC 4258

P. COX
Institut d'Astrophysique Spatiale, Université de Paris XI, F-91405 Orsay, France, and Institut d'Astrophysique de Paris, 92 bis, Boulevard Arago, F-75014 Paris, France

AND

D. DOWNES
Institut de Radio Astronomie Millimétrique, F-38406 St. Martin d'Hères, France

Received 1996 February 29; accepted 1996 July 2

ABSTRACT

We present CO (2–1) maps of the molecular gas associated with the inner parts of the anomalous arms of NGC 4258. The CO emission is found to be well correlated with the arms, and it extends out to $\sim$2 kpc from the center. Together with CO (1–0) and (3–2) measurements and the detection of ^{13}CO (1–0) and CS (3–2) toward the center of NGC 4528, we derive the physical conditions of the molecular gas along these arms and analyze in detail the dynamics of the gas. The molecular gas is relatively dense (10^3 cm^{-3} on average) and warm (50–100 K), with a total H_2 mass of 10^9 $M_\odot$. The CO distribution shows a characteristic S-shaped morphology, along which the molecular gas is found to move *toward* the nucleus, not away from it.

Contrary to previous interpretations, we suggest that the anomalous arms in NGC 4258 trace the gas flow due to a bar rather than being the manifestation of a jet. Both the S-shaped morphology and the velocity dispersion revealed by the present CO measurements are characteristic of barred galaxies. In the bar of NGC 4258, most of the gas is molecular, not atomic. The molecular gas is bounded by the sharp leading edge traced in the radio continuum that is probably the bar shock with its compressed magnetic field. The shocked Hα emission along the anomalous arms is probably a secondary manifestation of the bar shock. In the X-ray–emitting gas associated with the anomalous arms, the temperature is consistent with velocities and densities in bar-shock fronts rather than in jets of radio galaxies. We suggest that the X-rays, like the radio continuum and optical line emission, are produced via the bar shock and are unrelated to a jet from the black hole. The large extension of both the Hα and radio emission out to a projected distance of $\sim$7 kpc probably trace the hot (10^6 K) thermal X-ray gas produced by the bar shocks, which leaks out of the bar structure and eventually escapes from the disk in the z-direction. We predict that, with sufficient sensitivity and angular resolution, similar radio and X-ray emission will also be found in the shock fronts of other, more distant, barred galaxies.

Subject headings: galaxies: individual (NGC 4258) — galaxies: ISM — galaxies: kinematics and dynamics — galaxies: structure — radio lines: galaxies

1. INTRODUCTION

The galaxy NGC 4258 (M106) is well known for its anomalous Hα and nonthermal radio arms, apparently perpendicular to the normal spiral arms (Courtès & Cruvellier 1961; van der Kruit, Oort, & Mathewson 1972). The absence of beads of H II regions or a blue starlight continuum or near-UV continuum in the anomalous arms shows that the Hα-emitting gas is not excited by OB stars (Courtès & Cruvellier 1961; Courtès et al. 1993). The line ratios indicate excitation in shocks (van der Kruit 1974; Cecil, Morse, & Veilleux 1995a). The anomalous arms emerge from the middle of the galaxy as nearly straight features and then bend at 2–5 kpc radius in the trailing sense relative to the galactic rotation. The central $\pm 60''$ of the anomalous arms are in the galactic disk, because they contain a large mass of molecular gas (10^9 $M_\odot$; Krause et al. 1990)—far too much to be halo gas—and because the anomalous arms' Hα velocity centroids trace the disk rotation; the arms are rotating, not being ejected at an angle to the disk (van der Kruit 1974; Cecil, Wilson, & Tully 1992). Table 1 lists the global characteristics of the anomalous arms along with some of the main parameters of the galaxy.

Previous models have taken the ultimate origin of the anomalous arms to be ejection from the galaxy's nucleus. In the original model, the anomalous arms were supposed to trace the interaction between disk gas and gas expelled from the nucleus in an east-west direction in a single, gigantic explosion of energy 10^{57} ergs (van der Kruit et al. 1972). This expulsion model encountered serious difficulties with the results of Krause et al. (1990), who detected CO (1–0) in the center of NGC 4258 and *along* the anomalous arms to radii of 2 kpc from the center. These results showed that the molecular gas is closely related to the anomalous arms' Hα emission. The CO surface density is more than 10 times lower in the two radio continuum plateaus that trail the anomalous arms—that is, in the inner $r < 2$ kpc, there is no "normal" rotating disk with molecular gas, there are only the anomalous arms. The H_2 gas mass was estimated to be 3×10^8 $M_\odot$ in each of the anomalous arms out to 2 kpc from the center and 4×10^8 $M_\odot$ in the central region, yielding a total H_2 mass of 1×10^9 $M_\odot$. This large quantity of molecular gas along the anomalous arms shows that the expulsion model of van der Kruit et al. (1972) cannot be correct. The original model already needed an enormous energy, but the mass revealed by the CO is at least 10 times higher than in the model, making it even more unlikely on energetic grounds that the gas clouds detected in CO could have been expelled from the nucleus.

TABLE 1

NGC 4258 GALACTIC PARAMETERS

Parameter	Value	Reference
Galaxy:		
Morphological type	SAB(s)b	1
Distance	6.4 Mpc (1″ ↦ 31 pc)	2
Inclination (90° = edge-on)	72°	3
Position angle of major axis	150° E of N	3
Position angle of bar	145° E of N	4
L_{IR} (whole galaxy)	$1.2 \times 10^{10}\ L_\odot$	5
Nucleus:		
H_2O maser (B1950)	$12^h16^m29^s.369$, 47°34′53″.11	6
L_{IR} (central 6″)	2.2×10^{42} ergs s^{-1}	7
$L_{2-10\ keV}$	2.4×10^{40} ergs s^{-1}	8
Anomalous arms:		
Radius to bend points	90″ ↦ 2.6 kpc	9
$L_{H\alpha}$	9×10^{39} ergs s^{-1}	10
$L_{0.1-2.4\ keV}$	2×10^{40} ergs s^{-1}	10
$L_{mech}(gas) = MV^3/R$	3×10^{42} ergs s^{-1}	4
$L_{mech}(stars) = MV^3/R$	$>3 \times 10^{43}$ ergs s^{-1}	4

REFERENCES.—(1) de Vaucouleurs 1959; (2) Miyoshi et al. 1995; (3) van Albada 1980; (4) this paper; (5) Rice et al. 1988; (6) Greenhill et al. 1995; (7) extrapolated from 10 μm: Rieke & Lebofsky 1978; Cizdziel, Wynn-Williams, & Becklin 1985; (8) Makishima et al. 1994; (9) van der Kruit et al. 1972; (10) Cecil et al. 1995b.

The preferred current model has been continuous ejection in a jet. Interferometer observations of CO near the nucleus (Martin et al. 1989) and Hα studies (Ford et al. 1986; Cecil et al. 1992) were interpreted in terms of a jet's boring a channel in the interstellar medium with high-velocity gas streaming outward along braided helices. The X-rays from the anomalous arms were taken as further evidence of a jet (Cecil et al. 1992; Pietsch et al. 1994). However, the jet model is probably also wrong, because of the recent VLBI observations of H_2O masers, which have been interpreted as evidence for a black hole at the center of NGC 4258. The masers' distribution and kinematics indicate a mass of $3.6 \times 10^7\ M_\odot$ within a radius of less than 0.13 pc (Miyoshi et al. 1995; Greenhill et al. 1995). An important finding is that the maser disk is oriented *east-west*, and hence any jet from the black hole accretion disk should emerge in the north-south direction on the sky. Therefore an interaction with galactic disk gas should carry the jet into the northeast and southwest quadrants—the *opposite* of what is observed for the anomalous arms. The accretion rate of the maser/black hole disk is estimated to be $7 \times 10^{-5}\ M_\odot\ yr^{-1}$ (Moran et al. 1995; Neufeld & Maloney 1995). For equal accretion and mass-loss rates, the mass ejected during 10^7 yr, the estimated age of the anomalous arms in the jet model (e.g., Cecil, Wilson, & De Pree 1995b), would be only 700 $M_\odot$—completely negligible in comparison with the $10^9\ M_\odot$ in the arms' molecular gas. Even if all the ejected mass were in a 10,000 km s^{-1} jet, the mechanical power in the jet would be only 10^{38} ergs s^{-1}—5 orders of magnitude too low to produce observable kinematic effects on the massive molecular clouds. In our opinion, these maser results shed an entirely new light on the anomalous Hα and nonthermal radio arms in NGC 4258. We now suggest that these arms may be unrelated to any central black hole, that they probably do not trace a jet from the nucleus, and that their morphology, nonthermal radio emission, Hα filaments, and X-ray emission may all be by-products of the strong shocks in the flow of the molecular gas in the galaxy's bar.

2. OBSERVATIONS AND RESULTS

To study the dynamics of the molecular gas and its relation to the hotter gas, we mapped the anomalous arms of NGC 4258 in CO (1–0) and (2–1) with the IRAM 30 m telescope on Pico Veleta, near Granada, Spain. We observed simultaneously the CO (1–0) and (2–1) lines while the 2 mm receiver was tuned to the CS (3–2) line. A long integration was also performed on the ^{13}CO (1–0) line at the center of the galaxy. The telescope's beam at CO (2–1) is 12″.5. Pointing was checked by observations of planets and quasars and by CO (2–1) measurements at ±5″ around the nucleus of NGC 4258. Errors were less than 3″. The SIS receivers had receiver temperatures of ∼130 K at all three frequencies. The central region of the galaxy was sampled every 6″. A filter bank of 512 × 1 MHz channels yielded a velocity resolution of 2.6 km s^{-1} at 230 GHz, but for analysis we smoothed the spectra to a resolution of 10.4 km s^{-1}. Data were taken with a wobbling secondary with a 4′ throw in azimuth and were fitted with linear baselines.[1]

Additional measurements in CO (3–2) were made at selected positions along these arms at the Caltech Submillimeter Observatory, on Mauna Kea, Hawaii. The single-sideband SIS receiver temperature was 125 K, and the system temperature at 345 GHz was 1000 K (T_{mb}). The beam size at CO (3–2) is 22″. A filter bank of 1024 × 0.56 MHz channels yielded a velocity resolution of 0.49 km s^{-1} at 345 GHz. The data were subsequently smoothed to a resolution of 4.9 km s^{-1}. Pointing and calibration were accomplished by observing planets and strong nearby sources.

Figure 1*a* shows the spectra of the ^{12}CO (3–2), (2–1), and (1–0) lines at the center of the galaxy, and Figure 1*b* displays the spectra of the ^{13}CO and CS (3–2) lines. Table 2 sum-

[1] All spectral data in this paper are in main-beam brightness temperature (T_{mb}), as a function of LSR velocity corrected for the standard solar motion. To obtain heliocentric velocities (radio definition), subtract 8.1 km s^{-1}.

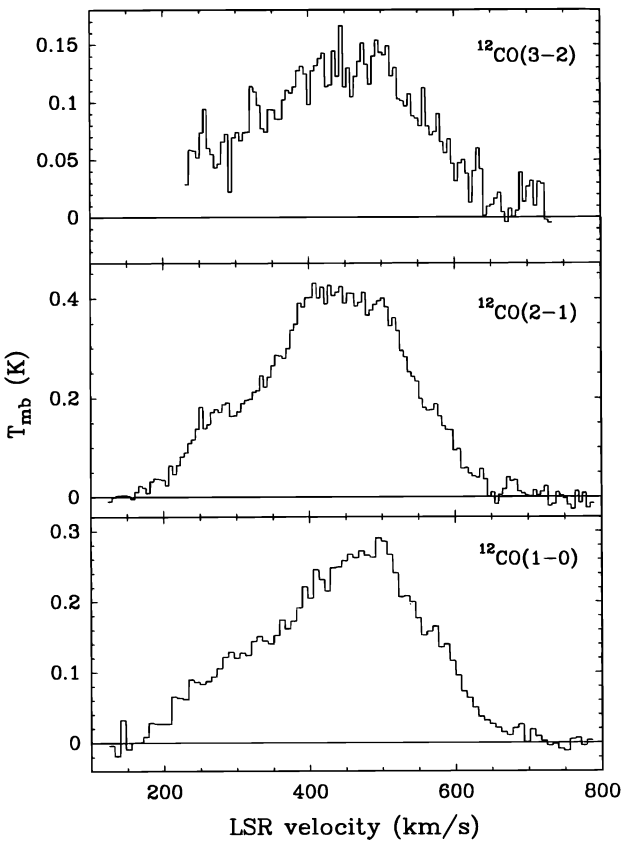

FIG. 1a

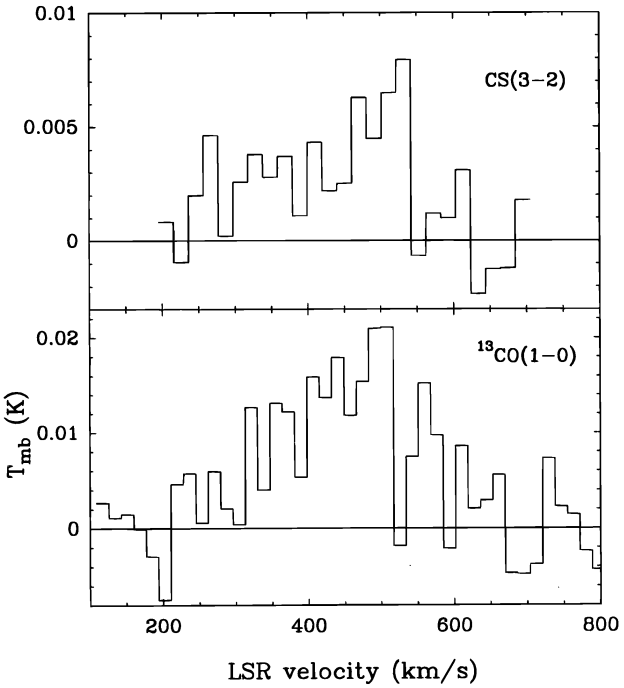

FIG. 1b

FIG. 1.—Spectra at the nucleus of NGC 4258 in (*a*) ^{12}CO (3–2), (2–1), and (1–0) (see Table 2) and in (*b*) CS (3–2) and ^{13}CO (1–0)

marizes the parameters of the CO lines at the nucleus of NGC 4258. In all transitions, the line centroid at the center of the galaxy is at 460 ± 10 km s^{-1}. The half-intensity line width is ~250 ± 20 km s^{-1}, and to the 20% level, the line widths are ~400 km s^{-1}. The total CO intensity, integrated over the CO (1–0) map, corresponds to an H_2 mass of $1 \times 10^9\ M_\odot$, in agreement with previous results (Krause et al. 1990). Figure 2 shows the CO (3–2) spectra at the five observed positions along the anomalous arms out to radii of 40″ from the nucleus. The spectra were taken with a wobbling secondary, and no baselines were subtracted from the raw data, which are shown in Figure 2. The CO (3–2) spectra show the variation of both the line widths and center velocity along the anomalous arms.

2.1. *Maps and Kinematics*

Figure 3 (Plate 1) presents the CO (2–1) maps in 60 km s^{-1} channels, superposed on the Hα image of Martin et al.

TABLE 2

CO LINE RESULTS

Parameter	CO (1–0)	CO (2–1)	CO (3–2)	^{13}CO (1–0)
Telescope:				
FWHM beamwidth (arcsec)	21	12.5	22	21
Point source S/T_{mb} (Jy K^{-1})	4.5	6.7	47	4.5
Intensities:[a]				
Peak flux density, S_{pk} (Jy)	1.2	3.9	6.1	0.072
Peak temperature, T_{mb} (K)	0.26	0.58	0.13	0.016
Peak flux, $\int S_{pk}\,dv$ (Jy km s^{-1})	320	770	1600	21
Peak $I_{CO} \equiv \int T_{mb}\,dv$ (K km s^{-1})	73	115	34	3.7
Peak I_{CO} convolved to 21″ (K km s^{-1})	73	72	34	3.7
Total flux, $\iint S\,dv\,d\Omega/\Omega_b$ (Jy km s^{-1})	1570	5440	...	...
Luminosity and H_2 mass:[b]				
L'_{CO} center (K km s^{-1} pc^2)	8×10^7	8×10^7	6×10^7	6×10^6
L'_{CO} center+arms (K km s^{-1} pc^2)	2×10^8	1×10^8	...	...
$M(H_2)$ center[c] ($M_\odot$)	4×10^8	...	...	...
$M(H_2)$ center+arms ($M_\odot$)	1×10^9	...	...	...

[a] At peak position; CO (2–1) line temperature and integrated intensity both peak at $(\Delta\alpha, \Delta\delta) = (-6'', 0'')$ relative to the nucleus (see Table 1).

[b] $L'_{CO} \equiv D^2 \int I_{CO}\,d\Omega_r$, where $d\Omega_r$ is the integral over the CO (1–0) or (2–1) map.

[c] $M(H_2/L'_{CO(1-0)}) = 4.6\ M_\odot$ (K km s^{-1} pc^2)$^{-1}$.

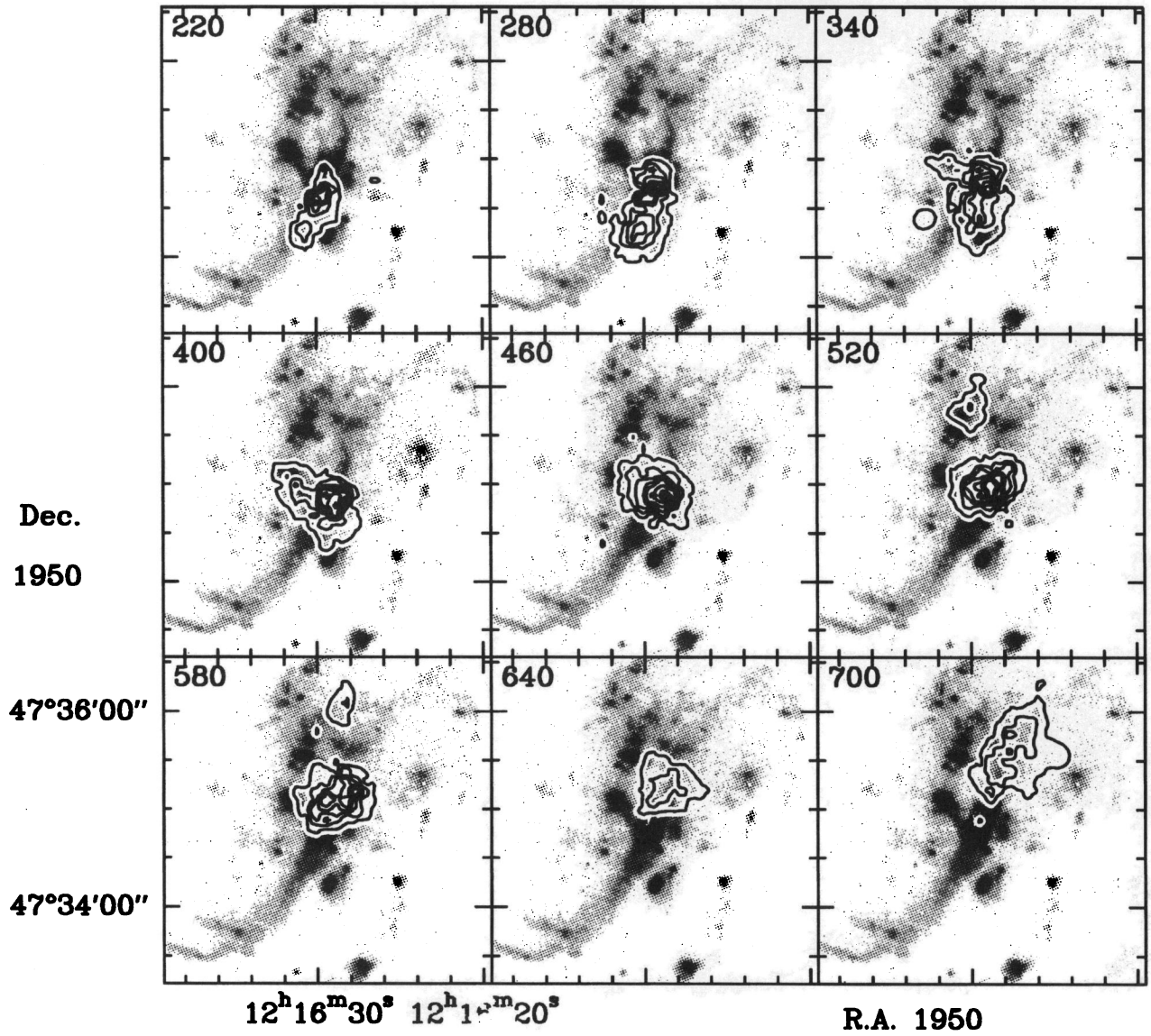

FIG. 3.—CO (2–1) in 60 km s^{-1} channels, superposed on an Hα CCD image (Martin et al. 1989). The FWHM beam is 12″.5 for CO (2–1), and the contour interval is 60 mK. Labels in the panels are LSR velocities in km s^{-1}.

Cox & Downes (see 473, 221)

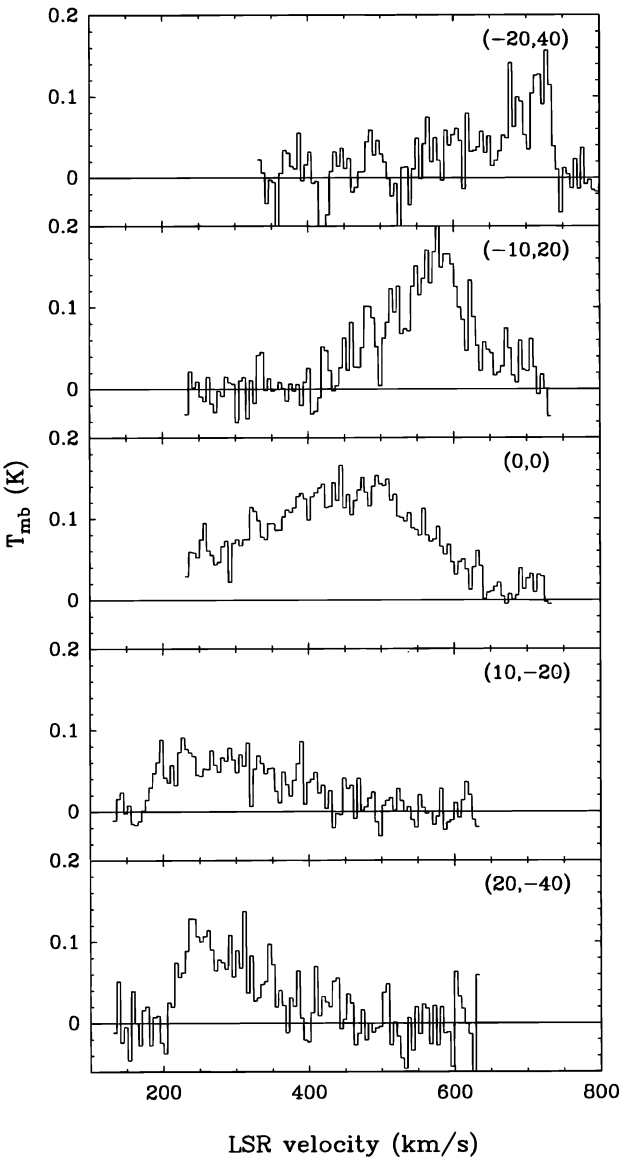

FIG. 2.—CO (3–2) spectra along the anomalous arms of NGC 4258, smoothed to a resolution of 4.9 km s^{-1}. Position offsets are relative to the nucleus (Table 1).

(1989). In the channel maps, the CO concentrations migrate from south to north with increasing radial velocity, as in the larger scale H I maps (van Albada 1980). However, in contrast to the H I, the CO is found entirely in the central region, where it follows the trace of the anomalous arms. Figures 4 and 5 show CO (2–1) position-velocity diagrams along (P.A. −30°) and normal to (P.A. +60°) the anomalous arms. The inflection points at ±20″ (~600 pc) from the nucleus are separated by 550 km s^{-1} (Fig. 4). Perpendicular to the anomalous arms (Fig. 5), two kinematic components are evident—the normal spiral arm component, with typically 100–200 km s^{-1} dispersion, extending to ±50″ normal to the anomalous arms, and the broad nuclear component that can be traced over a total of 600 km s^{-1} within ±10″ of the center.

Figure 6 shows the velocity-integrated CO (2–1) map superposed on the 6 cm VLA map of the radio continuum emission from P. Crane and S. Caganoff (see Cecil et al. 1995b) and the Hα image of NGC 4258 from Martin et al. (1989). The northwest and southeast CO ridges coincide well with the nonthermal radio continuum ridge. The CO ridges are slightly displaced from the Hα emission, with the CO leading the Hα emission in the sense of the galaxy's rotation. From the present data, there is no clear indication of a tunnel through the molecular clouds that might allow a jet of relativistic particles to pass freely, contrary to recent interpretations (see Cecil et al. 1995b; Plante et al. 1991).

The integrated CO map has the S-shaped pattern characteristic of the dust lanes of barred spirals, offset in parallel trails by ~20° relative to the major axis. If the CO and the radio continuum trace the lines of maximum compression of the gas, then in the sense of the galactic rotation, the Hα emission is *upstream* with respect to the CO and radio continuum ridges. At ±(20″–30″) from the nucleus, the Hα ridges are ~5″/cos *i*, or ~400 pc, upstream of the line of maximum density of the molecular gas and maximum compression of the magnetic field.

Figure 7 displays in greater detail the CO (2–1) integrated emission, the CO intensity-weighted isovelocity contours, and the CO velocity dispersion. The velocity contours show the typical S-shaped twist observed near the centers of barred galaxies. Given that the sense of rotation is counterclockwise and that the western side of the galaxy is the near side, it is clear that the gas in the CO ridges is moving toward the middle of the galaxy. The diagram of the velocity dispersion contours shows the central high-dispersion extension perpendicular to the major axis that is characteristic of barred galaxies. The sketch in Fig. 7*d* illustrates our suggested interpretation in terms of gas flows in a bar.

2.2. CO *Excitation;* CS *Detection*

To obtain line ratios, we convolved the CO (2–1) data to the same 21″ resolution as the CO (1–0) and CO (3–2) data. At the center of the galaxy, the CO (3–2):(2–1):(1–0) lines are in the proportion 0.45:1.0:1.0, and the $^{12}CO/^{13}CO$ ratio is 20 (Table 2). These ratios can be fitted by large velocity gradient modeling by relatively warm gas with a kinetic temperature of 50–100 K and an H_2 density of 1000 cm^{-3}, as in clouds in the centers of the Milky Way and other galaxies. For an observed CO (1–0) brightness temperature of 0.3 K and a predicted intrinsic brightness temperature of 30 K, the beam filling factor would typically be 0.01 for the brightest emission. Along the anomalous arms, the line ratios remain fairly constant, with CO (2–1)/(1–0) ≈ 1.0 and CO (3–2)/(2–1) ≈ 0.4. Thus the physical conditions appear to remain similar along the central ±60″ of the anomalous arms.

CS (3–2) emission was detected from the center of the galaxy, at a level of 0.005 K (Fig. 1*b*), corresponding to a ratio ^{12}CO (1–0)/CS (3–2) of 60. Sage, Shore, & Solomon (1990) found CO (1–0)/CS (2–1) ratios ranging from 20 to 80 in the centers of 11 nearby galaxies, and CS (3–2) may be slightly weaker than CS (2–1). Hence NGC 4258 may have a normal CS content and, hence, a normal ratio of dense (10^5 cm^{-3}) molecular gas (traced by CS) to diffuse (10^2–10^3 cm^{-3}) molecular gas (traced by CO).

3. EVIDENCE FOR THE ANOMALOUS ARMS' BEING A BAR PHENOMENON

On optical images, barred galaxies generally show a bright, oval-shaped inner region. The oval distortion in the central gravitational potential forces gas to stream in an S-shaped pattern (see, e.g., Athanassoula 1992). In the x_1-

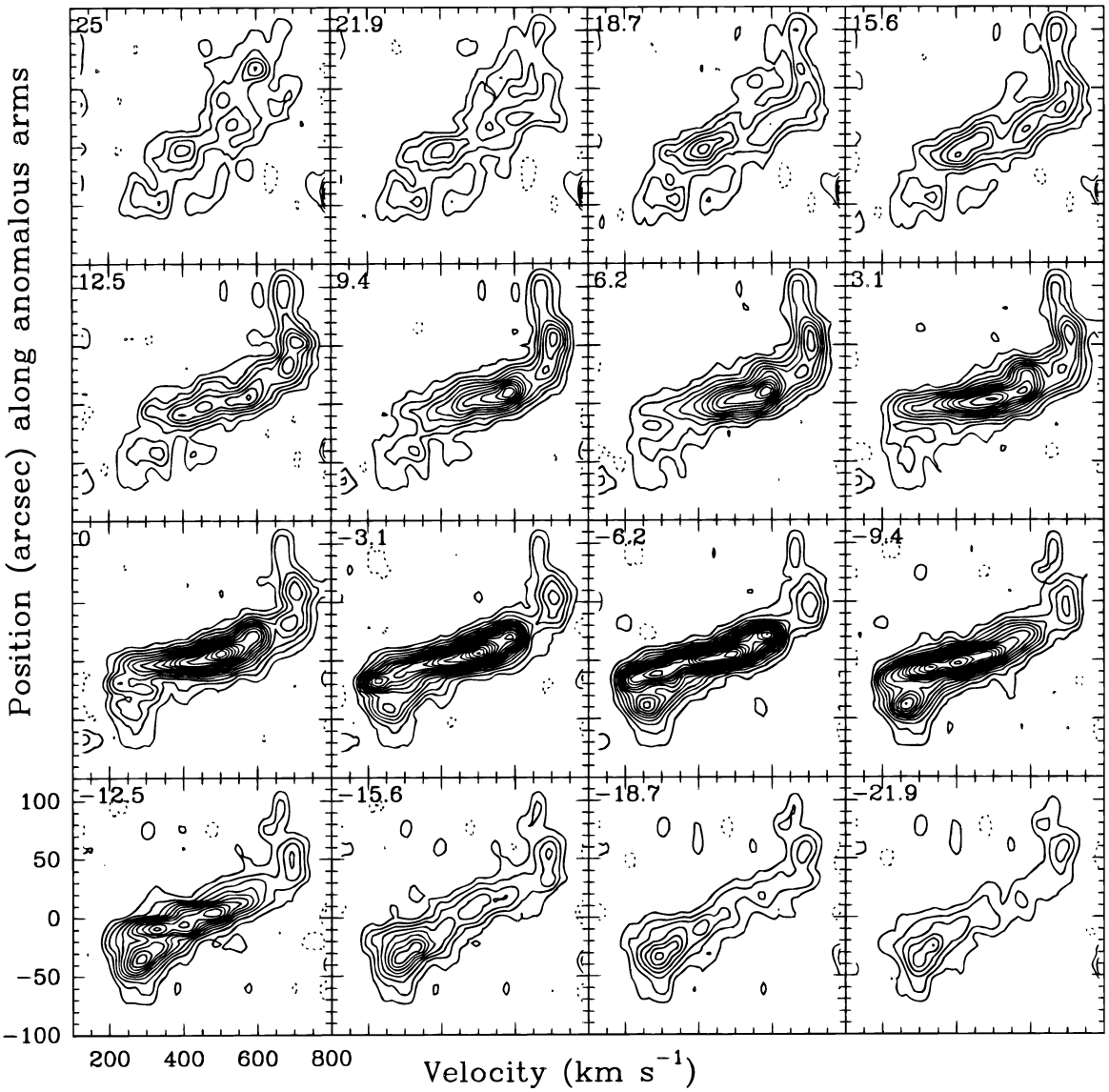

FIG. 4.—CO (2–1) position-velocity diagrams *parallel* to the anomalous arms (P.A. −30°). Labels (in arcseconds; upper left of each panel) are offsets perpendicular to the arms (east positive, west negative). The horizontal axis is LSR velocity in km s^{-1}, and the vertical axis is parallel to the anomalous arms. Northwest is at the top, southeast is at the bottom. The coordinate zero is the nucleus (Table 1). The contour interval is 25 mK; negative contours are dashed, zero contour omitted.

and x_2-orbit families (those along the bar and perpendicular to the bar, respectively) and at the x_1/x_2 interface at the center of the bar, the gas is mainly molecular (see, e.g., Downes et al. 1996). In barred galaxies, the gas along the dust-lane shocks moves inward, toward the nucleus. These inward motions are balanced by outward motions of much more tenuous gas beyond the shocks (see the flow patterns in, e.g., Athanassoula 1992). NGC 4258 was given by de Vaucouleurs (1959, p. 311) the classification SAB(s), which indicated an elongated nucleus crossed by a weak, twisted dark lane in the center of a weak, broad bar along an elongated lens that has much obscuring matter, tending to run parallel to the bar (see the sketch of NGC 4258 in de Vaucouleurs 1958).

The first kinematic evidence for a bar was found by Burbidge, Burbidge, & Prendergast (1963), who suggested that the ends of the bar could be at P.A. ~ 168°. Further kinematic evidence for a bar was found in the H I velocity pattern by van Albada & Shane (1975). Bosma (1978) modeled the H I velocity field and suggested that NGC 4258 could have been regarded as "the type example of an oval distortion (a bar) in a spiral galaxy." Bosma noted that the "gaps" in the Hα and H I images appeared to be associated with the Lagrangian points of the bar potential. From the integrated H I map, van Albada (1980) identified a barlike feature in the central region of the galaxy, at a position angle of 17°. However, this H I feature corresponds to the innermost parts of the northern spiral arm, well seen in the recent Hα images such as that in Figure 6*b*. We think a position angle of 140°–145° is more consistent with both the orientation of the CO and the starlight and extinction in the center of the galaxy. The elongation of the bright, central bulge along P.A. ~ 145° is nicely seen on the image published by Hubble (1943) and in the sequence of blue and red images of different exposure times published by Lindblad & Brahde (1946). We interpret the image of the 5000 Å/7000 Å ratio by Dutil, Beauchamp, & Roy (1995; their Figs. 3 and 4) as showing the orientation at

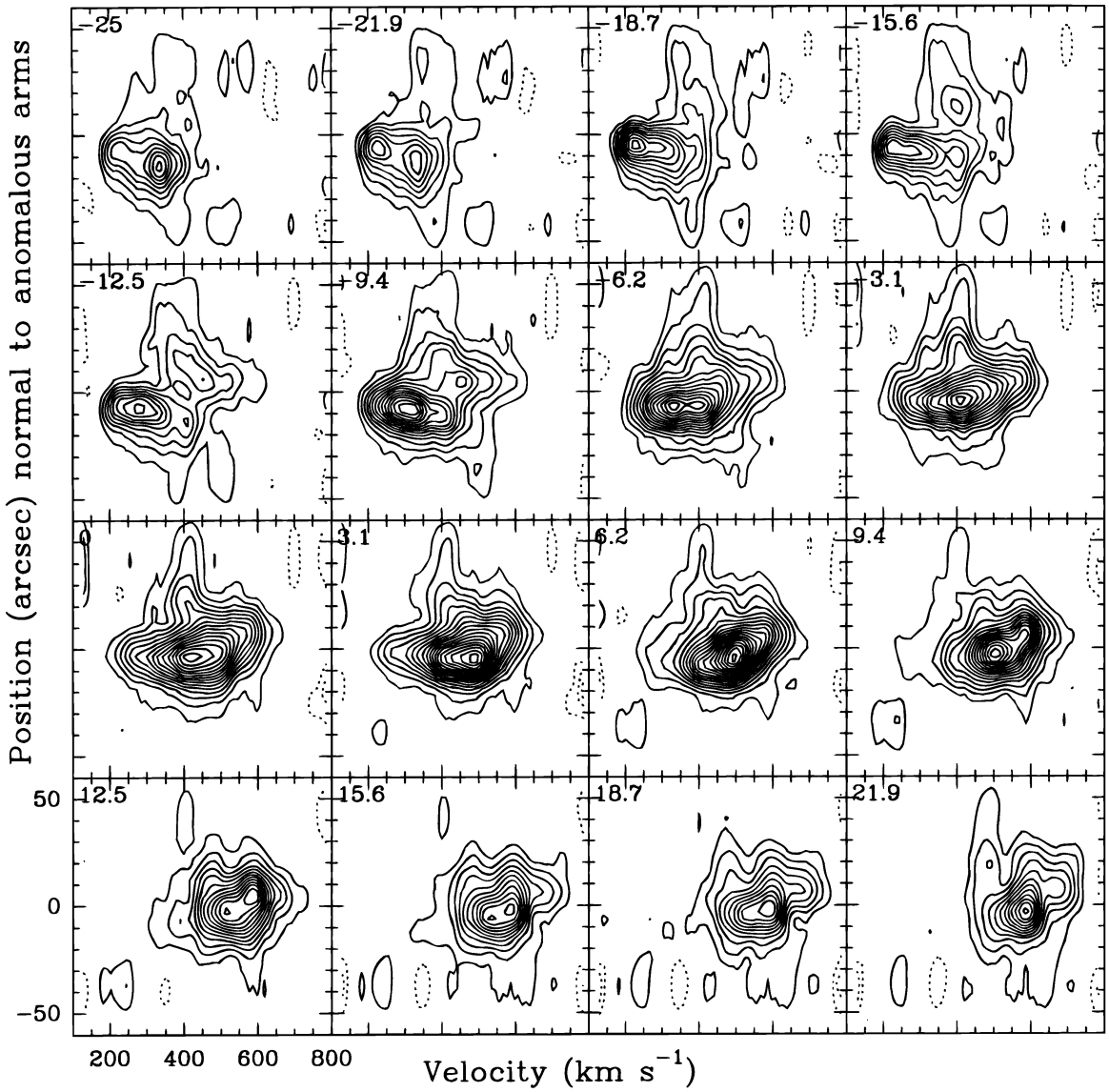

FIG. 5.—CO (2–1) position-velocity diagrams *perpendicular* to the anomalous arms (P.A. +60° east of north). Labels (in arcseconds; upper left of each panel) are offsets along the arms (southeast negative, northwest positive). The horizontal axis is LSR velocity in km s^{-1}, and the vertical axis is perpendicular to the anomalous arms. Northeast is up, and southwest is down. The coordinate zero is the nucleus (Table 1). The contour interval is 25 mK; negative contours are dashed, zero contour omitted.

P.A. ~ 145° of both the starlight along the bar—the light part of their image—and the near-side dust lane of the bar—the dark part of their image. Our CO map superposes nicely on the high-extinction part of their image.

The significance of the bar has been underestimated probably for two reasons. First, the bar is hard to see on optical images because of the 72° inclination of the galaxy and the near-coincidence of the bar with the major axis of the galaxy. Second, as shown by the present observations, most of the gas in the bar is molecular and was not detected in early H I studies. In the following sections, we will argue that the presence of a bar in the center of NGC 4258 can account for most of the known properties of the anomalous arms and that there is no need to invoke an ejection from the nucleus of the galaxy as in previous interpretations.

3.1. *Reasons Related to the Molecular Gas*

The gas mass is too high.—The mass of molecular gas along the anomalous arms (10^9 $M_\odot$) is too high to be explained by an expulsion model. The kinetic energy of a one-time expulsion at 1000 km s^{-1} would be a fantastic 10^{58} ergs, comparable with the rotational kinetic energy of *all* the matter—stars and gas—in the inner 4 kpc of the galactic disk! Rather than an expelled mass, the gas mass is typical of H_2 masses along galactic bars.

The molecular gas defines the inner parts of the anomalous arms.—The well-defined, smoothly symmetric pattern of molecular gas interior to $r = 2$ kpc (Fig. 6) cannot be reconciled with any expulsion model. Unlike the Hα and the radio continuum, which can be followed out to about $r = 7$ kpc, the CO is only seen in the inner parts of the "anomalous arms." Rather than defining the sharp edge of an outward-moving snowplow, the CO-emitting gas seems to nicely trace an elongated bar structure, interior to the hooks or bends in the anomalous arms.

The gas moves toward the nucleus, not away from it.—The CO isovelocity contours (Fig. 7) show that the radial component of motion in the anomalous arms is *toward* the

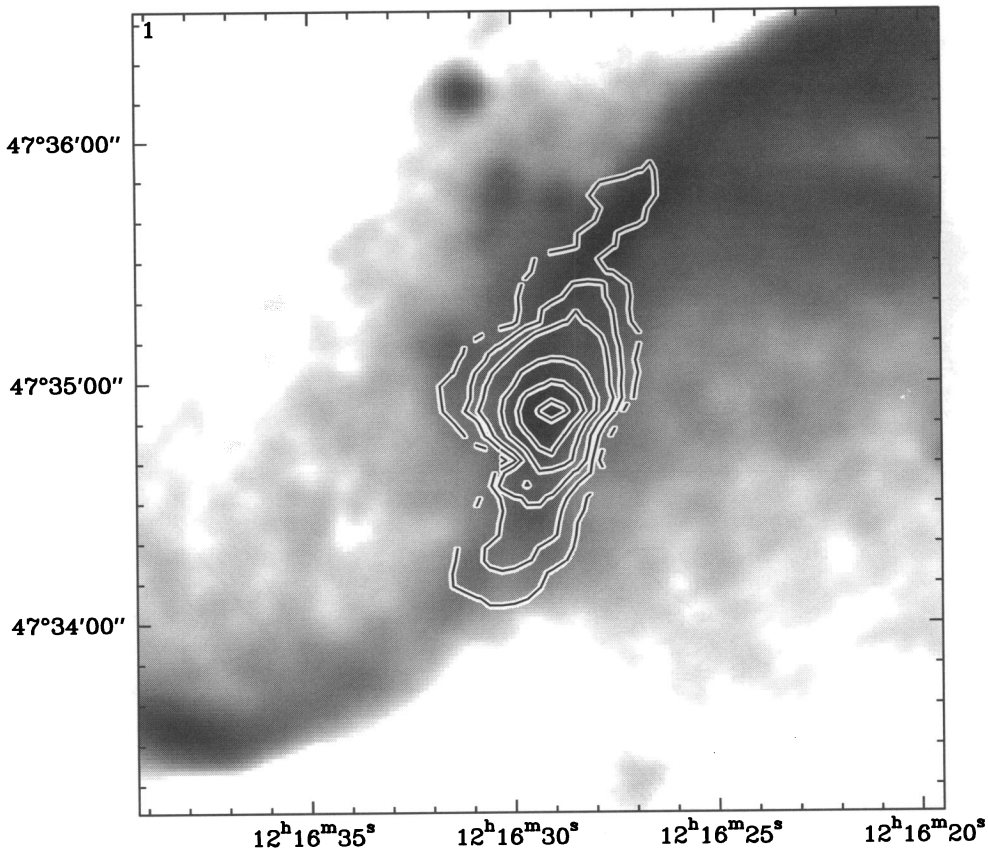

FIG. 6*a*

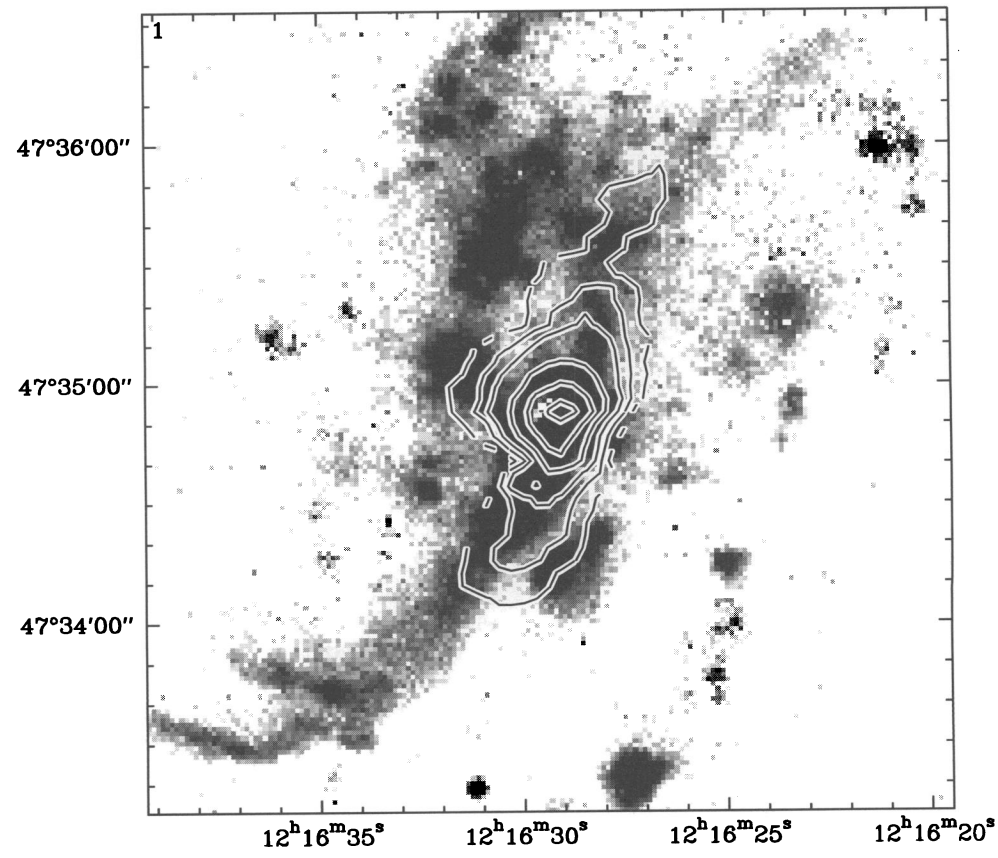

FIG. 6*b*

FIG. 6.—CO (2–1) integrated intensity over a 600 km s^{-1}–wide band centered on 450 km s^{-1}, superposed on (*a*) the 6 cm VLA radio continuum map of Crane and Caganoff and (*b*) the Hα image of Martin et al. (1989). Contours are 8, 20, 30, 50, 70, and 90 K km s^{-1}.

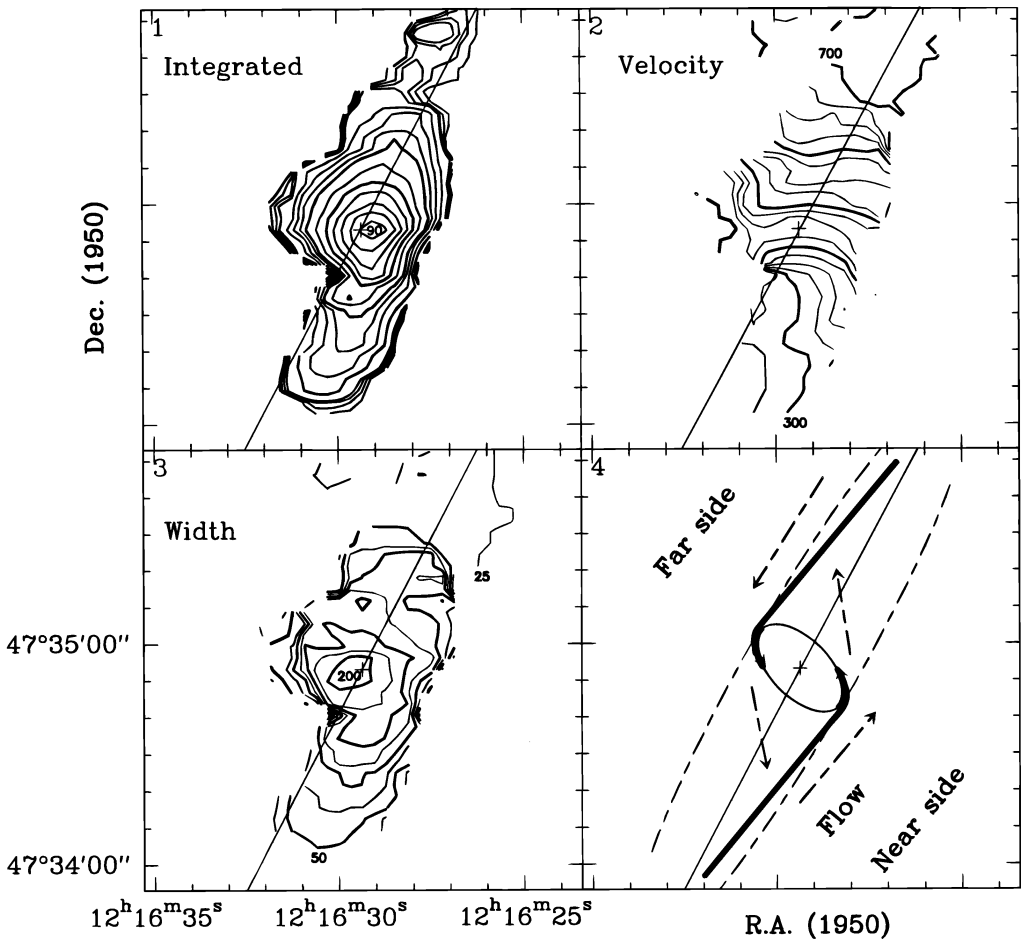

FIG. 7.—Summary of the CO distribution and kinematics in the inner parts of NGC 4258. In all panels, the cross marks the nucleus (Table 1). *Top left*: CO (2–1) integrated intensity over a 600 km s^{-1}–wide band centered on 450 km s^{-1}. Contours are 7, 8, 9, 10, then 15 to 30 in steps of 5 and 30 to 90 in steps of 10, in K km s^{-1}. *Top right*: Intensity-weighted isovelocity contours in steps of 25 km s^{-1}. The maximum is 712 km s^{-1}. *Bottom left*: Intensity-weighted contours of velocity dispersion in steps of 25 km s^{-1}. The maximum is 216 km s^{-1}. The cross marks the nucleus (Table 1). *Bottom right*: Interpretation of the molecular gas distribution as bar shocks. The arrows indicate a flow pattern derived from numerical simulations of bar gas flows (e.g., Athanassoula 1992). The diagonal line shows our interpretation of the axis of the bar of NGC 4258.

nucleus, exactly as is observed in the shocks of barred galaxies, not *away* from the nucleus as in a jet. This motion toward the nucleus was already found in the Hα velocity field mapped by van der Kruit (1974). Similar motion toward the nucleus was found in H I by van Albada & Shane (1975) and van Albada (1980), who were the first to interpret the kinematics as gas flow in a bar. In fact, the CO velocity pattern along the arms at P.A. 150° is consistent with gas flow along x_1-orbits. Near the center of the galaxy, and perpendicular to the anomalous arms, CO line widths become much greater, consistent with the existence of an x_2-orbit family.

3.2. *Reasons Related to the Optical Lines and X-Rays*

The Hα velocity pattern is consistent with bar motions.—The large jumps in Hα velocity near the nucleus are in the sense expected for the x_2-orbit family—see Figure 2 of Rubin & Graham (1990) and Figure 6 of Cecil et al. (1992). These velocity shifts can be interpreted as gas flow around an x_2-ring with radius 180 pc (sketch in Fig. 7), with gas approaching us with a large blueshift of $v_{lsr} - v_{sys} = 200 - 450 = -250$ km s^{-1} 5″ southeast of the nucleus and with gas receding from us at $600 - 450 = +150$ km s^{-1} 5″ northwest of the nucleus. The Hα spectra along P.A. 125° may be showing a mixture of approaching and receding x_1-orbit gas (near the x_1-cusps). Figure 12 of Cecil et al. (1992) shows that most of the Hα to the southeast is blueshifted, as would be expected for spray shock or dust-lane shear flow on this side of the galaxy. Farther down the southeast anomalous arm, the variations are more chaotic, but close to the center they are quite systematic. The systematic velocity shifts are probably due to the inclination of the Hα filaments relative to our line of sight.

Velocities in bar shocks are high enough to account for the X-rays.—An important point is that the bar-forming orbits cross the minor axis with very large streaming velocities that are much higher than the circular velocity for that radius. This explains the high spread of velocities observed in the Hα and the velocity of ~300 km s^{-1} needed to explain the 0.3 keV temperature deduced from the X-rays (Pietsch et al. 1994; Cecil et al. 1995b). The relevant velocity for the bar shock is the full 200–300 km s^{-1} velocity of the gas flow, not a computed velocity deviation relative to a circular rotation that in reality does not exist.

3.3. *Reasons Related to the Magnetic Field and Nonthermal Radio Emission*

The anomalous arms have steep leading edges in the sense of galactic rotation.—A nuclear jet rotating more slowly than disk gas—and acquiring angular momentum as disk

gas smashed into it—would have steep edges on the side *opposed to* the galactic rotation, exactly the contrary of what is observed: the steep front is in the sense of rotation, as is observed in the dust lanes that trace bar shocks.

The youngest electrons are at the shock front, at all radii.—The nonthermal radio emission in the anomalous arms has its lowest spectral index at the leading edge, *all along the length of the arms*, and not closest to the galactic nucleus (Hummel, Krause, & Lesch 1989). That is, the nonthermal spectral index steepens in the *azimuthal* direction, not radially outward from the nucleus. For a magnetic field of 20 μG, the steepening of the radio spectral index of the anomalous arms from -0.6 to -1.2 at a break frequency of 5 GHz implies a synchrotron lifetime of 2×10^7 yr (Hummel et al. 1989), i.e., comparable to or less than one galactic rotation period. These facts suggest the particles are accelerated on the spot, right at the leading edge of the anomalous arms, as expected for a bar shock.

There is no collimation, only a front.—Rather than being tightly collimated on both sides as in a tunnel, the nonthermal radio contours are steep only on the anomalous arms' leading edges in the sense of rotation, as expected if the magnetic field pattern is a feature of the bar shocks. Furthermore, since the magnetic field appears to be amplified on the leading edge of the anomalous arms, and since the relativistic electrons also appear to be accelerated there (see previous point), the nonthermal radio emission of the anomalous arms must have nothing to do with a jet from the nucleus. That is, the particles responsible for the nonthermal radio emission have not traveled along a tunnel through the molecular clouds. Conversely, without a cleared-out tunnel, there is too much resistance from the disk material for a jet to move outward from the nucleus. If there is no tunnel, there is no jet, on the scale implied by the anomalous arms.

There is no radio continuum VLBI source.—It is curious that there is no radio continuum source at the nucleus of NGC 4258 detectable by VLBI. With the full collecting area of the VLBA augmented by the full VLA, the 22 GHz upper limit on any flux at 1 mas resolution is 2 mJy (Miyoshi et al. 1995). It would be most unusual for a galaxy to have radio jets 5–10 kpc long without any source at the nucleus detectable by VLBI.

The real jet is much smaller.—The real radio jet, if there is one, from the black hole accretion disk may be the straight track close to the nucleus, seen on the VLA 6 cm map by Crane and Caganoff (see Cecil et al. 1995b, their Fig. 2*c*). This small jet seems to emerge for a distance of $\sim$1 kpc in the north-south direction—not east-west as in the original expulsion model of van der Kruit et al. (1972). The north-south direction is indeed perpendicular to the plane of the disk mapped in H_2O masers (Miyoshi et al. 1995). After traversing the distance of 1 kpc from the nucleus, the putative jet appears to be stopped in its tracks by the interstellar medium (Cecil et al. 1995a, 1995b).

3.4. *Comparison with Other Barred Galaxies*

Other barred galaxies have comparable H_2 *masses.*—The CO luminosity, and by inference the molecular gas mass, is typical of that in the centers of and along the bars of barred galaxies. Examples are $3 \times 10^8\ M_\odot$ in NGC 4314 (García-Barreto et al. 1991), $2 \times 10^8\ M_\odot$ in NGC 3351 (Devereux, Kenney, & Young 1992), $\sim 1 \times 10^9\ M_\odot$ in M101, NGC 6951, and NGC 3504 (Kenney et al. 1992), $2 \times 10^9\ M_\odot$ in M100 (Sakamoto et al. 1995), $6 \times 10^9\ M_\odot$ in the bar shocks in NGC 1365 (Sandqvist, Jörsäter, & Lindblad 1995), and $6 \times 10^9\ M_\odot$ in the bar shocks in NGC 1530 (Downes et al. 1996).

Other barred galaxies have Hα *from shocked gas along their bars.*—The high [N II]/Hα ratio and large velocity dispersion in the anomalous arms are similar to those in the line emission from bars of other galaxies, in which the high [N II]/Hα ratio along the bar also indicates shock excitation rather than photoionization by OB stars. Examples are NGC 1097 and 1672 (Storchi-Bergmann, Wilson, & Baldwin 1996), in which the shock-excited gas is well outside the nuclear rings. Another example may be Mrk 1066, in which the radio continuum and optical emission line "jets" are aligned along the galaxy's bar (Bower et al. 1995). These features may also delineate bar shocks rather than real jets from an active galactic nucleus. Numerous other barred galaxies also show [N II]/Hα ratios indicative of shock excitation (see, e.g., Burbidge & Burbidge 1965; Rubin, Ford, & Thonnard 1980; Duval 1977), which in retrospect should probably be reinterpreted as bar-induced shocks in the gas flow.

Smooth Hα emission without H II regions, similar to that in NGC 4258's anomalous arms, is also seen in NGC 3998 in an S shape extended over 7 kpc (Ford et al. 1986). This emission is similar to the anomalous arms in NGC 4258 in both the morphology and the [N II]/Hα ratio, which in this galaxy indicates shock ionization rather than photoionization by OB stars (Blackman, Wilson, & Ward 1983).

The barred galaxy NGC 6764 also shows the same phenomena: the same [N II]/Hα ratio (Boer & Schulz 1990), the same noncircular motions (Rubin & Graham 1987), and the same CO concentration (Eckart et al. 1991).

The nonthermal brightness temperature is the same as in the bars of other galaxies.—We may compare the 1.5 GHz brightness temperatures in NGC 4258's anomalous arms with those in other barred galaxies. NGC 4258's anomalous arms have $\sim$10–20 K in a 200 pc beam (van Albada & van der Hulst 1982). In NGC 1097, the bar shocks are 6 K in a 400 pc $\times$ 700 pc beam (Ondrechen & van der Hulst 1983; Hummel, van der Hulst, & Keel 1987). In NGC 1365, the bar shocks are 77 K in a 200 pc $\times$ 100 pc beam (Sandqvist et al. 1995). In M83, the bar shocks have $T_b \approx 6$–12 K in a 200 pc $\times$ 200 pc beam (Ondrechen 1985; Sukumar & Allen 1989). We suspect that, although not recognized as such, the radio continuum from the NGC 4258 bar shocks (i.e., the anomalous arms) was easily detected by van der Kruit et al. (1972) with $\sim$20″ beams because NGC 4258 is relatively nearby, while it is harder to detect radio continuum emission in the bar shocks of more distant barred galaxies. For example, in the bars of NGC 1097 and 1365, the nonthermal radio emission is only a few times the detection limit on the published VLA maps, even though the brightness temperature is the same as in the anomalous arms of NGC 4258. The reason is that, for more distant barred spirals, one must use smaller beams to have the same resolution in parsecs. However, the sensitivity, in T_b, deteriorates with (beamwidth)$^{-2}$, making it more difficult to detect features like NGC 4258's anomalous arms in distant barred galaxies.

Other barred galaxies have similar X-ray fluxes.—The extended thermal X-ray emission observed on a 45″ $\times$ 30″ scale around the bar of NGC 1566 has an X-ray luminosity in the 0.1–2.4 keV range of 1.4×10^{40} ergs s^{-1} (Ehle et al.

1996), about the same as that of the anomalous arms of NGC 4258. We suspect that the soft X-rays in NGC 1566 are also generated in bar-driven shocks. In NGC 5253, the luminosity of the 4×10^6 K thermal plasma is 7×10^{38} ergs s^{-1}. There also, the X-rays probably come from shocks in the gas flows (Martin & Kennicutt 1995).

4. DISCUSSION

We have argued here for a model in which the anomalous arms in NGC 4258 are probably the result of gas motions in a bar. We suggest that there are two phenomena: the inner parts of the anomalous arms, in the galactic disk and the bar itself, extending to a radius of 2.5 kpc from the nucleus; and the larger radio plateau regions in the shape of an S, extending to a projected radius of ~ 7 kpc.

The inner parts of the anomalous arms in NGC 4258 contain the dense molecular gas traced in CO and the strongest X-ray–emitting gas. Nearly all the properties derived for these inner parts are more easily interpreted as being due to the physics of gas flows and shocks in a barred galaxy rather than a jet. These properties include the molecular line emission, kinematics, and derived molecular mass, the strength of the radio continuum emission, the optical line ratios, velocity dispersions, the X-ray emission, the symmetric S-shaped morphology of the arms with a sharp leading edge in the direction of rotation, and the relation to the orientation of the H_2O maser disk. A bar explanation would also be consistent with the energies in the various components of the anomalous arms. Table 3 summarizes typical values for the bar properties in this interpretation. Such an interpretation has been difficult in the past because the high inclination of the galaxy makes the bar features look like a jet. The crucial new result is the information from the molecular gas, which shows most of the inner-galaxy gas is concentrated in the anomalous arms, exactly as in bar shocks.

The prominent bends at 2.5 kpc on the radio anomalous arms resemble the "hook" structure in the radio emission from the bar of NGC 1097 (Ondrechen & van der Hulst 1983). They may indicate the corotation radius at the end of the bar. We suggest that, near these bend points, the normal arms start in a two-armed spiral pattern. The situation would be like that in NGC 1097 and the prototypical barred spirals NGC 1300 and 1365. We illustrate our interpretation of NGC 4258 in Figure 8 (Plate 2), where we show the integrated CO contours—the location of most of the gas mass, the outermost VLA radio continuum contours, and the positions of H II regions cataloged by Courtès et al. (1993), on the basis of Hα images. We think the image that best shows the two-armed grand-design pattern is the UV continuum at 2000 Å (Courtès et al. 1993). We indicated in Figure 8 some of the peaks in the UV continuum as ellipses; at lower levels than these peaks, the UV light nicely traces the ridge lines of the outer spiral arms, shown as solid and dashed lines. It appears to us that the two-armed pattern starts near the ends of the bar (of which the CO probably traces the dust lanes). Each of the two arms then wraps around for $\geq 360°$, as is best seen in the UV images of Courtés et al. (1993; their Fig. 7) and as is also seen in many optical images of barred spirals.

TABLE 3

DERIVED QUANTITIES FOR THE ANOMALOUS ARMS

Parameter	Value	Note
Masses interior to $R = 2.5$ kpc ($M_\odot$):		
Hot gas mass, $m_X(10^6$ K)	$6 \times 10^4(1$ cm$^{-3}/n_e)$	1
H II mass	$2 \times 10^7(1$ cm$^{-3}/n_e)$	1
H_2 mass	1×10^9	2
Energy in arms (ergs):		
Relativistic particles	1×10^{54}	3
Magnetic field	1×10^{54}	3
Radiated in 10^7 yr	6×10^{54}	4
Molecular gas motion	8×10^{56}	2
Energy in the 10^6 K gas (ergs):		
Thermal energy, $L_X t_X$	2×10^{54}	5
Potential energy, GMm_X/r	2×10^{53}	6

NOTES.—(1) Cecil et al. 1995b; (2) this paper; (3) de Bruyn 1977; (4) energy radiated in optical lines and soft X-rays, from Table 1; (5) for X-ray gas cooling time $t_X = 4 \times 10^6$ yr, Cecil et al. 1995b; (6) for $M = 10^{10} M_\odot$ and $r = 2.5$ kpc.

Why does the radio continuum emission extend well beyond the CO distribution and appear to cross all the outer, "normal" spiral arms? The radio plateau regions, in our view, trace the locations where the hot (10^6 K) thermal X-ray gas that has been produced by the bar shocks leaks out of the bar structure and eventually escapes from the disk in the z-direction. Evaporation from the disk is likely, because, in the hot gas, the thermal energy exceeds the gravitational potential energy (Table 3). This escaping hot gas partakes in the rotation of the galaxy and trails the bar in an extended S shape. Similar cones of hot gas may be flowing out of the bar and disk of NGC 1097. (See the images by Wolstencroft & Zealey 1975, Arp 1976, and Lorre 1978, where the four "rays" have been interpreted as jets. We think it more likely that the "rays" are the boundaries of the hot gas outflow cones.)

The apparent crossing of this component of the anomalous arms over the normal spiral arms is thus a projection effect, with the outer parts of the radio plateau emission actually above and below the galactic disk. Such an interpretation agrees with the polarization of the radio emission in the anomalous arms observed by Hummel et al. (1989). There is no polarization in the anomalous arms from the nucleus out to a radius of 2 kpc, consistent with an origin in the plane of the galaxy. In contrast, the radio plateau emission at larger galactocentric radii is polarized. On the eastern plateau, at positions 1 to 4 of Hummel et al., the depolarization parameter (DP, the ratio of the polarization percentage at 1.5 and 4.9 GHz) varies between 1.0 and 0.6, which indicates there is little depolarization and suggests that this emission is above the plane of the galaxy. On the western plateau, at positions 7 to 10 of Hummel et al., there is significant depolarization (DP = 0.1–0.3), indicating this emission is below the plane of the galaxy.

An important consequence of the proposed interpretation of the anomalous arms in terms of gas flow due to a bar is that NGC 4258 is one of the few nearby galaxies in which the bar-shock phenomenon can be studied with high linear resolution. The energetics (Table 3) and the radiant luminosities (Table 1) imply that the kinetic energy of the gas flow in the bar can be dissipated by radiation at a relatively high rate—1% every 10 million years. This high radiative loss rate has not yet been incorporated in numerical simulations of bar flows. The example of NGC 4258 indicates that bar shocks have a high luminosity in visible lines and X-rays. In galaxies at large distances, this radiation might be mistaken for that of active galactic nuclei and lead to classifications as "LINER nuclei" (see also the discussion

PLATE 2

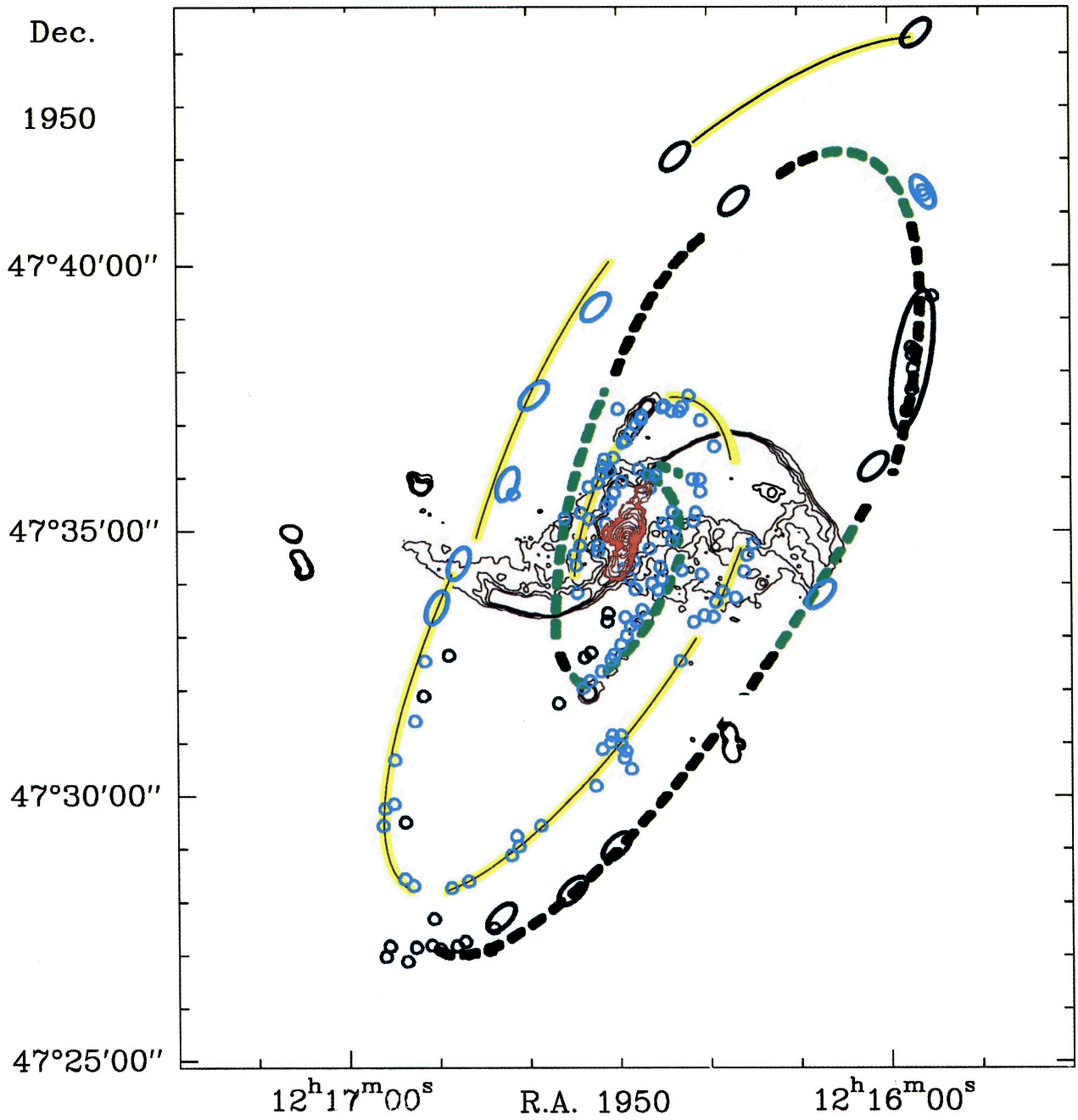

FIG. 8.—Our interpretation of the relation of the bar in NGC 4258 (the inner parts of the anomalous arms) to the normal spiral arms. The red contours show our map of the integrated CO (2–1) emission, which indicated the location of most of the central gas mass, and probably trace the dust lanes of the bar. The black contours show the 0.2, 0.3, 04, and 0.5 mJy beam^{-1} levels on the 6 cm VLA radio continuum map by Crane and Caganoff. The small blue circles show the H II regions cataloged by Courtès et al. (1993) from Hα images. The blue ellipses show local maxima in the UV light at 2000 Å (Courtès et al. 1993). The solid yellow and dashed green lines show our best estimate of the ridge lines of the two-armed grand-design spiral pattern traced by the UV light at 2000 Å (Courtès et al. 1993).

COX & DOWNES (see 473, 228)

of ionization by shocks in Morse, Raymond, & Wilson 1996). The example of NGC 4258 shows that the shocks that yield the characteristic LINER ratios may be generated in the orbital motions of the near-nuclear gas ($r \approx 1$ kpc), and not by a central black hole.

We thank P. Crane, S. Caganoff, and G. Cecil for providing the VLA continuum data. We are grateful to Y. Dutil, P. Martin, J. R. Roy, R. Plante, and K. Y. Lo for the Hα data, and to M. Bremer for reformatting the Hα data. We thank A. Bosma, F. Combes, and N. Neininger for useful discussions. We also thank R. Bachiller for help at the IRAM 30 m telescope and K. Young for help during the CSO observations, which were partly supported by NSF grant AST 93-13929 to the California Institute of Technology.

REFERENCES

Arp, H. C. 1976, ApJ, 207, L147
Athanassoula, E. 1992, MNRAS, 259, 345
Blackman, C. P., Wilson, A. S., & Ward, M. J. 1983, MNRAS, 202, 1001
Boer, B., & Schulz, H. 1990, Ap&SS, 163, 201
Bosma, A. 1978, Ph.D. thesis, Univ. Groningen
Bower, G., Wilson, A., Morse, J. A., Gelderman, R., Whittle, M., & Mulchaey, J. 1995, ApJ, 454, 106
Burbidge, E. M., & Burbidge, G. R. 1965, ApJ, 142, 634
Burbidge, E. M., Burbidge, G. R., & Prendergast, K. H. 1963, ApJ, 138, 375
Cecil, G., Morse, J. A., & Veilleux, C. 1995a, ApJ, 452, 613
Cecil, G., Wilson, A. S., & De Pree, C. 1995b, ApJ, 440, 181
Cecil, G., Wilson, A. S., & Tully, R. B. 1992, ApJ, 390, 365
Cizdziel, P. J., Wynn-Williams, C. G., & Becklin, E. E. 1985, AJ, 90, 731
Courtès, G., & Cruvellier, P. 1961, CR Acad. Sci. Paris, 253, 218
Courtès, G., Petit, H., Hua, C. T., Martin, P., Blecha, A., Huguenin, D., & Golay, M. 1993, A&A, 268, 419
de Bruyn, A. G. 1977, A&A, 58, 221
de Vaucouleurs, G. 1958, ApJ, 127, 487
———. 1959, in Encyclopedia of Physics, ed. S. Flügge, Vol. 53 (Berlin: Springer), 53, 275
Devereux, N. A., Kenney, J. D. P., & Young, J. S. 1992, AJ, 103, 784
Downes, D., Reynaud, D., Solomon, P. M., & Radford, S. J. E. 1996, ApJ, 461, 186
Dutil, Y., Beauchamp, D., & Roy, J. R. 1995, ApJ, 444, L85
Duval, M. F. 1977, Ap&SS, 48, 103
Eckart, A., Cameron, M., Jackson, J. M., Genzel, R., Harris, A. I., Wild, W., & Zinnecker, H. 1991, ApJ, 372, 67
Ehle, M., Beck, R., Haynes, R. F., Vogler, A., Pietsch, W., Elmouttie, M., & Ryder, S. 1996, A&A, 306, 73
Ford, H. C., Dahari, O., Jacoby, G. H., Crane, P. C., & Ciardullo, R. 1986, ApJ, 311, L7
García-Barreto, J. A., Downes, D., Combes, F., Gerin, M., Magri, C., Carrasco, L., & Cruz-González, I. 1991, A&A, 244, 257
Greenhill, L. J., Jiang, D. R., Moran, J. M., Reid, M. J., Lo, K. Y., & Claussen, M. J. 1995, ApJ, 440, 619
Hubble, E. 1943, ApJ, 97, 112
Hummel, E., Krause, M., & Lesch, H. 1989, A&A, 211, 266
Hummel, E., van der Hulst, J. M., & Keel, W. C. 1987, A&A, 172, 32
Kenney, J. D. P., Wilson, C. D., Scoville, N. Z., Devereux, N. A., & Young, J. S. 1992, ApJ, 395, L79
Krause, M., Cox, P., García-Barreto, J. A., & Downes, D. 1990, A&A, 233, L1
Lindblad, B., & Brahde, R. 1946, ApJ, 104, 211
Lorre, J. J. 1978, ApJ, 222, L99
Makishima, K., et al. 1994, PASJ, 46, L77
Martin, C. L., & Kennicutt, R. C., Jr. 1995, ApJ, 447, 171
Martin, P., Roy, J.-R., Noreau, L., & Lo, K. Y. 1989, ApJ, 345, 707
Miyoshi, M., Moran, J., Herrnstein, J., Greenhill, L., Nakai, N., Diamond, P., & Inoue, M. 1995, Nature, 373, 127
Moran, J., Greenhill, L., Herrnstein, J., Diamond, P., Miyoshi, M., Nakai, N., & Inoue, M. 1995, Proc. Natl. Acad. Sci., 92, 11427
Morse, J. A., Raymond, J. C., & Wilson, A. S. 1996, PASP, 108, 426
Neufeld, A. A., & Maloney, P. R. 1995, ApJ, 447, L17
Ondrechen, M. P. 1985, AJ, 90, 1474
Ondrechen, M. P., & van der Hulst, J. M. 1983, ApJ, 269, L47
Pietsch, W., Vogler, A., Kahabka, P., Jain, A., & Klein, U. 1994, A&A, 284, 386
Plante, R. L., Lo, K. Y., Roy, J. R., Martin, P., & Noreau, L. 1991, ApJ, 381, 110
Rice, W., Lonsdale, C. J., Soifer, B. T., Neugebauer, G., Koplan, E. L., Lloyd, L. A., de Jong, T., & Habing, H. J. 1988, ApJS, 68, 91
Rieke, G. H., & Lebofsky, M. J. 1978, ApJ, 220, L37
Rubin, V. C., Ford, W. K., & Thonnard, N. 1980, ApJ, 238, 471
Rubin, V. C., & Graham, J. A. 1987, ApJ, 316, L67
———. 1990, ApJ, 362, L5
Sage, L. J., Shore, S., & Solomon, P. M. 1990, ApJ, 351, 422
Sakamoto, K., Okumura, S., Minezaki, T., Kobayashi, Y., & Wada, K. 1995, AJ, 110, 2075
Sandqvist, Aa., Jörsäter, S., & Lindblad, P. O. 1995, A&A, 295, 585
Storchi-Bergmann, T., Wilson, A. S., & Baldwin, J. A. 1996, ApJ, 460, 252
Sukumar, S., & Allen, R. J. 1989, Nature, 340, 537
van Albada, G. D. 1980, A&A, 90, 123
van Albada, G. D., & Shane, W. W. 1975, A&A, 42, 433
van Albada, G. D., & van der Hulst, J. M. 1982, A&A, 115, 263
van der Kruit, P. C. 1974, ApJ, 192, 1
van der Kruit, P. C., Oort, J. H., & Mathewson, D. S. 1972, A&A, 21, 169
Wolstencroft, R. D., & Zealey, W. J. 1975, MNRAS, 173, 51P

Note added in proof.—J. Moran (Center for Astrophysics, Cambridge, Massachusetts) informs us that a VLBI continuum source has been found at the nucleus of the galaxy at a level of 1.8 mJy at 22 GHz.